ACCRUAL OF OSTEOCLAST PRECURSORS DRIVES BONE LOSS AFTER DENOSUMAB DISCONTINUATION: A DIGITAL TWIN STUDY

Charles Ledoux[1], Daniele Boaretti[1], Jack J. Kendall[1] , Ralph Müller[1], Caitlyn J. Collins[1,2]

[1]Institute for Biomechanics, ETH Zurich, Zurich, Switzerland, [2]Virginia Tech, Blacksburg, United States

Introduction

Incidence of osteoporosis (OP) is increasing with our aging population. Denosumab, a common treatment for OP, is a monoclonal antibody that binds to RANKL and thus reduces osteoclastogenesis, osteoclast-mediated bone resorption and remodeling rates. Upon cessation of treatment, however, resorption rises quickly to levels higher than baseline and rapid bone loss occurs [1]. This has been attributed to: blocked differentiation and thus accumulation of (A) osteoclast precursors [2] or (B) osteomorphs, cells in the marrow originating from the fission of osteoclasts on the bone surface [3], (C) low osteoblast numbers leading to a higher RANKL/OPG ratio upon evacuation of denosumab than prior to treatment or (D) increased sclerostin production by osteocytes to return to the pre-treatment mechanostat setpoint. We quantify the relative contributions of these mechanisms to the withdrawal effect using an in-house micro-multiphysics agent-based (micro-MPA) model that generates digital twins of patient iliac crest biopsies.

Methods

For the micro-MPA model, bone and marrow cells are represented as agents on a voxel-based lattice and are motile and capable of producing or resorbing tissue and signaling molecules [4]. A micro-multiphysics solver is used to determine the diffusion, decay and reactions of signaling molecules (Fig. 1A). Concomitantly, the bone mechanical environment is simulated using micro-finite element analysis to determine the internal strains, which serve as stimulus for the osteocytes and osteoblasts. Starting from micro-computed tomography (micro-CT) scans of iliac crest biopsies (n=7) from postmenopausal women (age: 72±5 years) [4] simulation runs for 2 years of treatment followed by 2 years of discontinuation were executed based on four different versions of the model each isolating one of the mechanisms proposed in literature.

Results

All mechanisms lead to an increase in BMD during treatment followed by a drop during discontinuation (Fig. 1C). During treatment, the osteomorph and RANK/OPG ratio mechanisms best represented the clinical treatment data, with the other mechanisms overestimating the change in BMD. The sclerostin only mechanism failed to accurately represent the treatment phase of the clinical data and resulted in a premature drop in BMD. After treatment, the osteomorph mechanism best represented the initiation of denosumab withdrawal, but overestimated the total loss in BMD at two years post-discontinuation. In contrast, the simulations based on the accumulation of osteoclast precursors yielded a more conservative initiation of withdrawal, but better represented the long-term stabilization of the BMD in the clinical cohort.

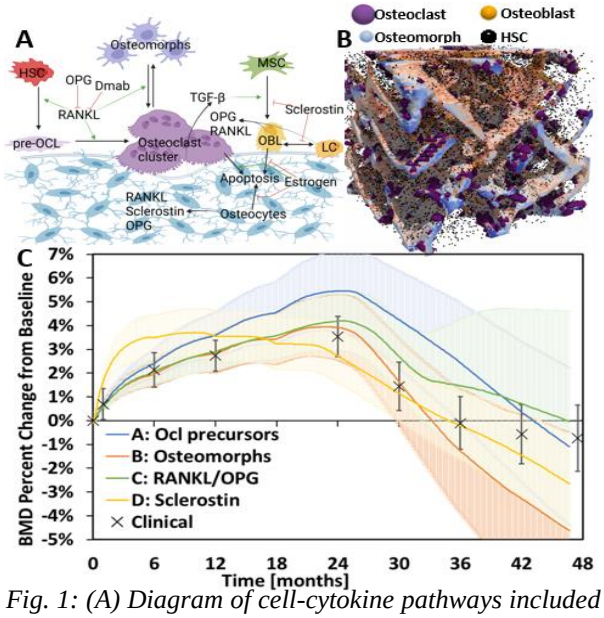

Fig. 1: (A) Diagram of cell-cytokine pathways included in micro-MPA model, (B) initial distribution of key cell types on 3-D biopsy and (C) bone mineral density trends

Discussion

Our study suggests that both accumulation of preosteoclasts and osteomorphs play a key role in the cell-cytokine dynamics following denosumab discontinuation, with accumulation of preosteoclasts contributing approximately twice as many resurgent osteoclasts as osteomorphs but osteomorphs playing a role faster. Future work will include performing equivalence tests not only with the individual mechanisms but also with combinations of these to quantify contributions. This study demonstrates that micro-MPA models provide a fast and inexpensive tool to computationally test hypotheses relating to bone mechanobiology and may assist in formulating *in silico* trials to help reduce and refine human clinical trials targeting alternative strategies for OP treatment and sequencing of available pharmaceuticals.

References

1. Bone et al. (2011) J Clin End & Met 96(4):972-80
2. Fontalis et al. (2020) Bone Reports 13:100457
3. McDonald et al. (2021) Cell 184(5):1330-1347
4. Tourolle et al. (2021) JBMR Plus 5(6):e10494

Acknowledgements

Support from the Swiss National Supercomputing Centre (project s1070) and the Euler compute cluster at ETH Zurich.